

# Supporting Information

Deng et al. 10.1073/pnas.1409354111

## SI Materials and Methods

**Reagents.** The cDNA of human ADAM10 was purchased from Addgene. The vectors and strains for the AraTM assay have been previously described (1, 2). Restriction enzymes were purchased from New England Biolabs. Thrombin, glutathione 4B Sepharose beads, and the Superdex 200 10/300 column were purchased from GE Healthcare. Trypsin from the bovine pancreas was purchased from Sigma-Aldrich. H-Lys(Z)-OtBu-HCl, tert-butyl bromoacetate, 5(6)-carboxyfluorescein n-hydroxysuccinimide ester (NHS-FS), and 5(6)-carboxytetramethylrhodamine n-hydroxysuccinimide ester (NHS-TMR) were purchased from Sigma Aldrich. *N*-dodecylphosphocholine and other phospholipids were purchased from Avanti Polar Lipids.

**Expression and Purification of A10Cp, A10TmCp, and Derivatives.** The DNA fragment encoding the cytoplasmic domain of ADAM10 (residues Lys697–Arg748) or the transmembrane-cytoplasmic domains of ADAM10 (residues Leu666–Arg748) was amplified from the cDNA of ADAM10, appended with a sequence encoding a C-terminal hexahistidine tag when desired, and subcloned as a BamHI/XhoI fragment into the pHex vector (3). Expression of the GST-fusion protein in *E. coli* BL21 cells and its purification was carried out as described previously (4, 5). Removal of the GST protein by thrombin cleavage and further purification of A10Cp, A10Cp-6H, or A10TmCp-6H was performed following the published protocols (3–5). Although A10TmCp-6H contains an intact transmembrane helix, it is water soluble after the HPLC purification. Both proteins could be directly dissolved in the DPC micellar solution (20 mM Tris-HCl, 10 mM DPC, 100 mM NaCl, and 1 mM DTT, pH 8.0) and was stored at 4 °C before use. The concentrations of the protein samples were determined using the BCA protein assay kit (Pierce Biotechnology).

**Phospholipid Modification of A10Cp.** Maleimide-mediated conjugation of 1,2-dipalmitoyl-sn-glycero-3-phosphoethanolamine-*N*-[4-(*p*-maleimidomethyl)cyclohexane-carboxamide] (DiPal) to residue Cys699 of A10Cp or A10Cp-6H in an organic-based solvent was performed following the previously published protocol (6). The DiPal-conjugated protein was purified by reverse-phase HPLC and lyophilized into powder and stored at –80 °C before use. Its purity and identity was confirmed by HPLC, SDS/PAGE, and MS. Neither DiPal-A10Cp nor DiPal-A10Cp-6H is water soluble. To make the stock solution of lipidated protein, 1 mg of DiPal-conjugated protein powder was dissolved into 1 mL DPC micellar solution by extensive vortex. The final protein concentration was determined using the BCA protein assay kit.

**Reconstitution of A10TmCp-6H in POPC Liposomes.** The reconstitution of A10TmCp-6H in the POPC liposome was performed following the previously published protocol (5). Briefly, 100  $\mu$ L of 2.1 mg/mL A10TmCp-6H dissolved in ethanol was mixed with 300  $\mu$ L of 10 mg/mL POPC in chloroform (a molar ratio of 1/200) and gently dried to a thin film under a stream of nitrogen gas. After being vacuumed overnight, the dried film was rehydrated and resuspended in 2 mL of 20 mM Tris-HCl, 100 mM NaCl, and 1 mM DTT, pH 8.0. The mixture was converted to large unilamellar vesicles using a miniextruder device (Avanti Polar Lipids) with a 400-nm pre-sized filter. The concentration of A10TmCp-6H in the POPC liposome was determined using the BCA protein assay kit.

**CD Spectroscopy.** The protein was diluted using the DPC micellar solution or a buffer otherwise specified to the final concentration

of 40  $\mu$ M. The far-UV CD spectra (190–260 nm) of the protein samples were collected on a JASCO J810 spectrometer using a 0.1-cm quartz cuvette at 20 °C. The stepwise wavelength was set to 0.2 nm/step. Each spectrum was averaged after 10 scans and corrected for background signal (buffer without the protein).

**Trypsin Digestion.** The protein stock solution was diluted to the final concentration of 100  $\mu$ g/mL using DPC micellar solution or a buffer otherwise specified. An aliquot of 100  $\mu$ L protein was mixed with 1  $\mu$ L of 0.5 mg/mL trypsin dissolved in DPC micellar solution or a buffer otherwise specified. The mixture was incubated at 37 °C for 1 h followed by inactivation at 95 °C for 5 min. Then 20  $\mu$ L of the digestion mixture was loaded into a reverse-phase C4 column and analyzed in an Agilent 1260/6100 LC/MS instrument at 20 °C. The mass spectrometer was operated in full-scan mode with a resolution of 10,000.

**Chemical Synthesis of Fluorescein-tri-NTA and TMR-tri-NTA.** Tri-NTA (*t*-Bu)<sub>3</sub> was synthesized according to the published protocol (7). To make fluorophore-tri-NTA, 1 mg NHS-FS or NHS-TMR was mixed with 0.5 mg tri-NTA(*t*-Bu)<sub>3</sub> in 80% (vol/vol) chloroform/20% (vol/vol) methanol. The reaction was kept in the dark for 6 h at room temperature. The product was separated from the excess NHS-fluorophore via silica gel column chromatography. The collected product was concentrated to 1 mL and further treated with 10 mL of 95% (vol/vol) TFA to remove the *t*-butyl group. The mass spectrum of each product was obtained on a Voyager DE-STR MALDI-TOF spectrometer in the Mass Spectrometry Center at Emory University. The purified products were dissolved in 20 mM Tris-HCl, pH 8.0, buffer with the individual concentration being determined based on the respective extinction coefficients (80,000 M<sup>-1</sup>·cm<sup>-1</sup> at 490 nm for FS and 78,000 M<sup>-1</sup>·cm<sup>-1</sup> at 548 nm for TMR).

**Fluorescence Anisotropy Titration.** Fluorescence anisotropy titrations were performed on a polarizer-equipped PTI QuantaMaster spectrometer (Photon Technology International) using a 3-mL quartz cuvette. Each fluorophore-tri-NTA was diluted individually to DPC micellar solution or a buffer otherwise specified to the final concentration of 1 nM. During the measurement, 10–100  $\mu$ L aliquots of protein samples were titrated into the fluorophore-tri-NTA solution. The excitation wavelengths were set to 494 nm for FS-tri-NTA and 540 nm for TMR-tri-NTA, with both slit widths at 5 nm. The fluorescence anisotropy at any given protein concentration was measured as previously described (8) and averaged over three independent measurements. The titration data were plotted as anisotropy vs. the protein concentration. The equilibrium dissociation constant,  $K_{\text{NTA}}$ , was obtained by fitting the titration plot to a hyperbolic binding equation (5).

**FRET Measurements.** To measure the steady-state fluorescence spectra, 1  $\mu$ L of 10  $\mu$ M FS-tri-NTA and 100  $\mu$ M TMR-tri-NTA was added, individually or jointly, to either 1 mL DPC micellar solution containing 1  $\mu$ M NiSO<sub>4</sub> or the same solution that contained 200 nM of the desired protein. Fluorescence emission of each sample was recorded for 505–650 nm on the aforementioned PTI instrument, with the excitation wavelength at 494 nm and both slit widths at 3 nm. In each measurement, the final emission spectrum was averaged from three individual scans and corrected for the buffer background.

**Determination of the Oligomeric State of A10TmCp-6H in DPC Micelles by FRET.** Unlabeled tri-NTA and TMR-tri-NTA, both of which were prepared in the same DPC micellar solution to the stock

concentration of 10  $\mu\text{M}$ , were added in various combinations to 1 mL of DPC micellar solution that also contained 200 nM A10TmCp-6H and 100 nM FS-tri-NTA. The overall tri-NTA concentration was kept constant at 200 nM in all samples. Each FS emission intensity at 520 nm was averaged from eight individual scans using a 1-nm step size and 1-s integration time and corrected for buffer background. The excitation wavelength was 494 nm with both slit widths at 3 nm. Quenching of the FS fluorescence intensity ( $F/F_0$ ) was plotted against the mole ratio of TMR-tri-NTA/FS-tri-NTA, where  $F_0$  is the FS fluorescence in the absence of TMR-tri-NTA.

**Determination of the Dimerization Constant ( $K_d$ ) of A10TmCp-6H by FRET.** A mixture of FS-tri-NTA and TMR-tri-NTA was prepared in the DPC micellar solution to a final concentration of 100  $\mu\text{M}$  for each fluorophore. The fluorophores were diluted 1,000-fold into either 1 mL of DPC micellar solution (as the no-quenching control) or 1 mL of the same solution containing 200 nM A10TmCp-6H. An aliquot of 200  $\mu\text{L}$  of each sample was transferred to a 96-well flat-bottom microtiter plate (Sigma) and was serially diluted by the DPC micellar solution. The FS fluorescence emission intensities of all of the diluted samples in the microtiter plate were recorded using a Synergy II fluorescence plate reader (BioTek), with excitation maximum at 485 nm and emission at 530 nm. At each concentration of A10TmCp-6H, the FRET efficiency ( $E$ ) was calculated as

$$E = 1 - F/F_0, \quad [\text{S1}]$$

where  $F$  and  $F_0$  were the measured fluorescence intensities of the A10TmCp-6H sample and the no-quenching control, respectively.

The following equations were derived to describe the linked equilibria of fluorophore-tri-NTA association with A10TmCp-6H and the dimerization of A10TmCp-6H. With the assumption that free FS-tri-NTA and A10TmCp-6H-bound FS-tri-NTA have the same mole fluorescence, the observed FS fluorescence intensity is given by

$$F_0 = \varepsilon[\text{FS}]_{\text{T}} = \varepsilon x/2, \quad [\text{S2}]$$

$$F = \varepsilon[\text{FS}]_{\text{U}} + \varepsilon(1 - E_{\text{max}})[\text{FS}]_{\text{Q}}, \quad [\text{S3}]$$

where  $\varepsilon$  is the mole fluorescence of FS-tri-NTA,  $[\text{FS}]_{\text{T}}$  represents the total moles of FS-tri-NTA,  $[\text{FS}]_{\text{U}}$  is the mole of unquenched FS-tri-NTA,  $E_{\text{int}}$  is the intrinsic FRET efficiency, and  $[\text{FS}]_{\text{Q}}$  is the mole of quenched FS-tri-NTA. Taking into account Eq. S4, we obtain Eq. S5

$$[\text{FS}]_{\text{T}} = [\text{FS}]_{\text{U}} + [\text{FS}]_{\text{Q}}, \quad [\text{S4}]$$

$$E = 1 - \frac{F}{F_0} = E_{\text{int}} \frac{[\text{FS}]_{\text{Q}}}{[\text{FS}]_{\text{T}}} = 2E_{\text{int}}[\text{FS}]_{\text{Q}}/x, \quad [\text{S5}]$$

where  $x$  is the total concentration of A10TmCp-6H. The dimerization of A10TmCp-6H can be described by Eqs. S6 and S7

$$K_d = \frac{[M]^2}{[D]}, \quad [\text{S6}]$$

$$[M] + 2[D] = x, \quad [\text{S7}]$$

where  $K_d$  is the dimerization constant,  $[M]$  is the concentration of the monomeric A10TmCp-6H, and  $[D]$  is that of the dimeric form. Therefore, from Eqs. S6 and S7, we obtain

$$[M] = \frac{-K_d + \sqrt{K_d^2 + 8xK_d}}{4}, \quad [\text{S8}]$$

$$[D] = \frac{x - [M]}{2} = \frac{4x + K_d - \sqrt{K_d^2 + 8xK_d}}{8}. \quad [\text{S9}]$$

When the concentration of total tri-NTA and the concentration of A10TmCp-6H is the same, the association of tri-NTA with A10TmCp-6H can be described by Eqs. S10 and S11

$$K_{\text{NTA}} = \frac{[\text{NTA}]^2}{[\text{NTA} \cdot \text{prot}]}, \quad [\text{S10}]$$

$$[\text{NTA}] + [\text{NTA} \cdot \text{prot}] = x, \quad [\text{S11}]$$

where  $K_{\text{NTA}}$  is the dissociation constant for NTA binding,  $[\text{NTA}]$  is the concentration of free tri-NTA, and  $[\text{NTA} \cdot \text{prot}]$  is the concentration of tri-NTA/A10TmCp-6H complex. Therefore, from Eqs. S10 and S11 we obtain

$$[\text{NTA}] = \frac{-K_{\text{NTA}} + \sqrt{K_{\text{NTA}}^2 + 4xK_{\text{NTA}}}}{2}, \quad [\text{S12}]$$

$$[\text{NTA} \cdot \text{prot}] = x - [\text{NTA}] = \frac{2x + K_{\text{NTA}} - \sqrt{K_{\text{NTA}}^2 + 4xK_{\text{NTA}}}}{2}. \quad [\text{S13}]$$

Because the dimerization of A10TmCp-6H and the association of tri-NTA with A10TmCp-6H use different sequences in the protein, we assume that the two reactions are independent of each other. Thus,  $[\text{FS}]_{\text{Q}}$  is proportional to both  $[D]$  and the percentage of bound tri-NTA in total tri-NTA. Because FS-tri-NTA and TMR-tri-NTA bound to A10TmCp-6H with the same affinity (Table 1), the distribution of FS-tri-NTA and TMR-tri-NTA in the bound tri-NTA population should be the same. Therefore,  $[\text{FS}]_{\text{Q}}$  can be expressed as

$$[\text{FS}]_{\text{Q}} = A[D][\text{NTA} \cdot \text{prot}]/x, \quad [\text{S14}]$$

where  $A$  is a coefficient that describes the distribution of FS-tri-NTA in the mixture. Taking into account Eqs. S9, S13, and S14, from Eq. S5 we obtain

$$E = E_{\text{int}} A \frac{\left(4x + K_d - \sqrt{K_d^2 + 8xK_d}\right)}{8x^2} \times \left(2x + K_{\text{NTA}} - \sqrt{K_{\text{NTA}}^2 + 4xK_{\text{NTA}}}\right). \quad [\text{S15}]$$

The plot of  $E$  vs.  $x$  (Fig. 4B) was fit to Eq. S15 by nonlinear least-squares global curve fitting using Igor Pro-6.21. It should be noted that, although DPC was included in the experiment, DPC concentration was kept constant throughout the serial dilution and fluorescence measurement. Because the dimerization is mediated by the cytoplasmic domain of ADAM10 in the aqueous solution, the dimerization constant was expressed in the unit of protein concentration rather than the protein/detergent mole fraction.

**AraTM Assay.** Expression plasmids encoding various MBP-TmCp-AraC proteins were cloned largely as described previously (1, 6). Each plasmid was cotransformed with pAraGFP plasmid into the AraC-deficient *E. coli* strain SB1676 and streaked on Luria Broth (LB) plates with 100  $\mu\text{g}/\text{mL}$  ampicillin and 50  $\mu\text{g}/\text{mL}$

kanamycin (1). For the DN-AraTM test, vectors encoding the AraC and DN AraC proteins were mixed in equal amount and transformed into *E. coli*. The transformed bacteria were cultured largely as previously described (1), and 30  $\mu$ L of each culture was diluted to 1 mL of selective LB media for the measurement of its optical density at 600 nm ( $OD_{600}$ ). For the measurement of GFP fluorescence, 300  $\mu$ L of each culture was transferred to a 96-well flat-bottom microtiter plate, and a series of 1.5-fold serial dilution was prepared using the selective LB media. The GFP fluorescence intensities (excitation maximum at 485 nm and emission maximum at 530 nm) were recorded using a Synergy II fluorescence plate reader. Results are plotted as the ratio of fluorescence emission at 530 nm to  $OD_{600}$  as described previously (1).

**Western Blot.** To detect the expression level of MBP fusion proteins in bacteria, the aforementioned bacterial cells were pelleted from the culture and lysed in 1/10 volume of lithium dodecyl sulfate sample buffer including the reducing agent (Invitrogen). The target proteins were resolved in a 12% (wt/vol) Bis-Tris SDS gel using the Mops running buffer (Invitrogen), transferred to nitrocellulose membrane, and blotted by anti-MBP monoclonal antibody (Sigma). The blots were visualized on a GeneGnome imaging instrument (Syngene) using HRP-conjugated goat anti-mouse IgG (Thermo Scientific) and Supersignal West Pico Luminal reagent (Thermo Scientific).

**MalE Complementation Test.** Equal amounts of pAraTM plasmids and pAraGFP were cotransformed into the MM39 cells and

streaked onto selective LB plates (100  $\mu$ g/mL ampicillin and 50  $\mu$ g/mL kanamycin) and incubated at 37 °C for 16 h. The positive colonies were cultured in the selective LB media overnight. The saturated culture from each construct was streaked on selective M9 minimal media plates (100  $\mu$ g/mL ampicillin) containing 0.4% (wt/vol) maltose as the only carbon source and incubated for 48 h at 37 °C to assess growth. The pMAL-c2 and pMAL-p2 plasmids that express MBP protein in the cytoplasm and periplasm, respectively, were included as controls.

**Inhibition of A10TmCp Dimerization.** In a flat-bottom 96-well microtiter plate, stocks of A10TmCp-6H, DiPal-A10Cp, A10Cp, and/or lysozyme (as negative control) were mixed to various molar ratios in the DPC micellar solution containing 100 nM FS-tri-NTA and 100 nM TMR-tri-NTA or in the same solution containing just 100 nM FS-tri-NTA. The final concentration of A10TmCp-6H was kept to 200 nM for all of the samples in the well. The plate was incubated at room temperature for 1 h before the FS fluorescence emission intensities at 530 nm were recorded using the aforementioned plate reader. The fluorescence readings after buffer background subtraction were averaged from four wells. The fluorescence readings of the samples containing both FS- and TMR-tri-NTA were considered as  $F$ , and those containing just FS-tri-NTA were  $F_0$ . The average of  $F/F_0$  obtained from three independent measurements was plotted against the peptide/A10TmCp-6H molar ratio.

1. Su PC, Berger BW (2012) Identifying key juxtamembrane interactions in cell membranes using AraC-based transcriptional reporter assay (AraTM). *J Biol Chem* 287(37):31515–31526.
2. Su PC, Berger BW (2013) A novel assay for assessing juxtamembrane and transmembrane domain interactions important for receptor heterodimerization. *J Mol Biol* 425(22):4652–4658.
3. Luo S-Z, et al. (2007) Glycoprotein I $\alpha$  forms disulfide bonds with 2 glycoprotein I $\beta$  subunits in the resting platelet. *Blood* 109(2):603–609.
4. Deng W, Cho S, Li R (2013) FERM domain of moesin desorbs the basic-rich cytoplasmic domain of I-selectin from the anionic membrane surface. *J Mol Biol* 425(18):3549–3562.
5. Deng W, Srinivasan S, Zheng X, Putkey JA, Li R (2011) Interaction of calmodulin with L-selectin at the membrane interface: Implication on the regulation of L-selectin shedding. *J Mol Biol* 411(1):220–233.
6. Srinivasan S, Deng W, Li R (2011) L-selectin transmembrane and cytoplasmic domains are monomeric in membranes. *Biochim Biophys Acta* 1808(6):1709–1715.
7. Huang Z, Park JI, Watson DS, Hwang P, Szoka FC, Jr (2006) Facile synthesis of multivalent nitrilotriacetic acid (NTA) and NTA conjugates for analytical and drug delivery applications. *Bioconjug Chem* 17(6):1592–1600.
8. Luo SZ, Li R (2008) Specific heteromeric association of four transmembrane peptides derived from platelet glycoprotein Ib-IX complex. *J Mol Biol* 382(2):448–457.

**A**  
 A10Cp-6H: GSGGGKICSVHTPSSNPKLPPPKPLPGTLKRRRPPQPIQQPPRQRPRESYQMGHMRRHHHHHH  
 A10Cp: GSGGGKICSVHTPSSNPKLPPPKPLPGTLKRRRPPQPIQQPPRQRPRESYQMGHMRR  
 A10TmCp-6H: GSGGGLYENIAEWIVAHWWAVLLMGIALIMLMAGFIKICSVHTPSSNPKLPPPKPLPGTLKRRRPPQPIQ  
 QPPRQRPRESYQMGHMRRHHHHHH

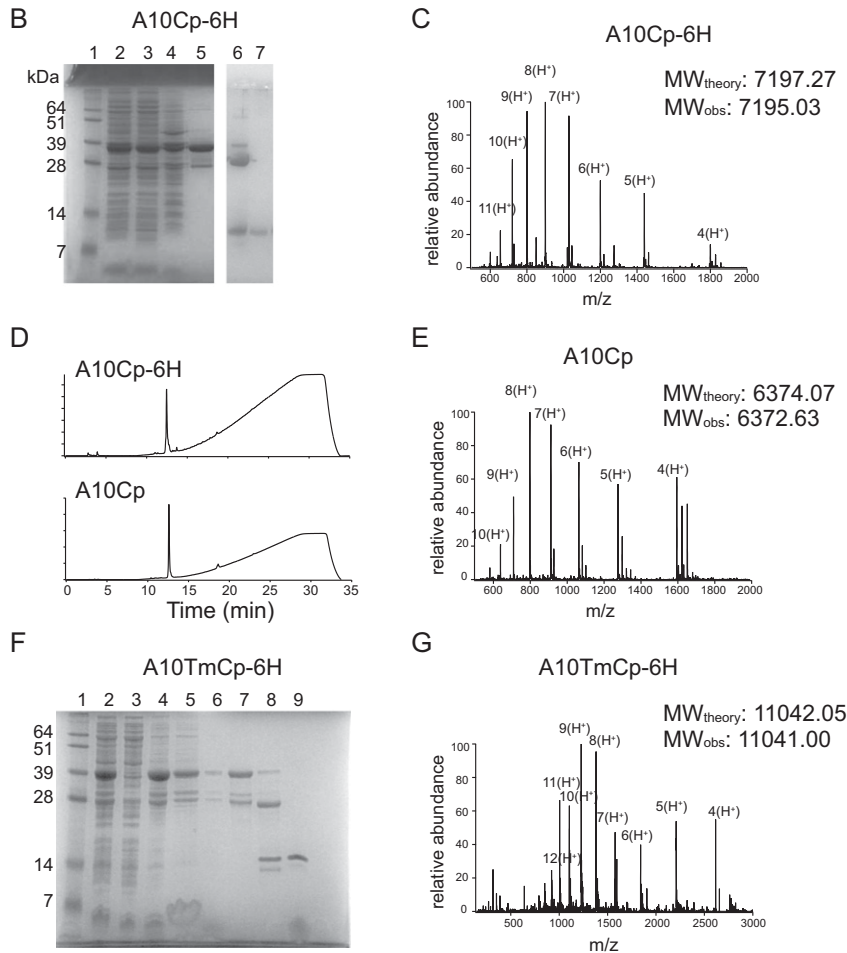


**Fig. S1.** Expression and purification of ADAM10-derived recombinant proteins. (A) Amino acid sequences of ADAM10-derived proteins used in this study. (B) SDS gel depicting expression and purification of A10Cp-6H. Lane 1, molecular weight marker, with corresponding numbers marked on the left; lane 2, whole cell lysate; lane 3, supernatant from the lysate; lane 4, flow-through from the glutathione Sepharose 4B column; lane 5, 10H-GST-A10Cp-6H fusion protein eluted from the column; lane 6, thrombin cleavage to generate the 10H-GST fragment and A10Cp; lane 7, purified A10Cp-6H. A10Cp without the C-terminal hexahistidine tag was purified in the same way. (C and E) Mass spectra of A10Cp-6H and A10Cp to confirm their identities. (D) Overlaid analytical HPLC traces of purified A10Cp-6H and A10Cp. (F) SDS gel depicting expression and purification of A10TmCp-6H. Lane 1, molecular weight marker; lane 2, whole cell lysate; lane 3, lysate supernatant; lane 4, lysate pellet; lane 5, isolated inclusion body; lane 6, flow-through from the Ni-NTA column; lane 7, 10H-GST-A10TmCp-6H fusion protein eluted from the Ni-NTA column; lane 8, thrombin cleavage to generate the 10H-GST fragment and A10TmCp-6H; lane 9, A10TmCp-6H after HPLC purification. (G) Mass spectrum of purified A10TmCp-6H.

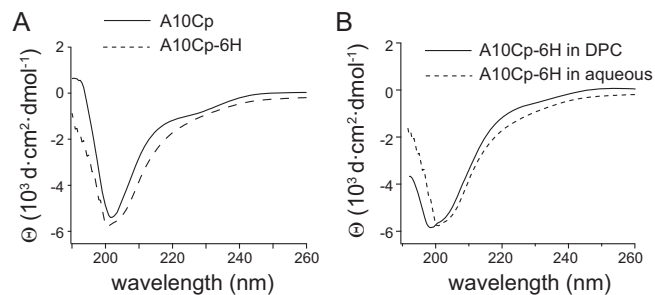


**Fig. S2.** Conformation of A10Cp assessed by CD spectroscopy. (A) Overlaid CD spectra of A10Cp-6H and A10Cp in aqueous solutions. Both proteins were dissolved in the 20 mM Tris-HCl buffer (containing 100 mM NaCl and 1 mM DTT, pH 8.0) to a final concentration of 40  $\mu\text{M}$ . Each spectrum was the average of 10 scans at 20  $^\circ\text{C}$ . (B) Overlaid CD spectra of A10Cp-6H in either the above aqueous solution or the solution also containing 10 mM DPC (DPC micellar solution).

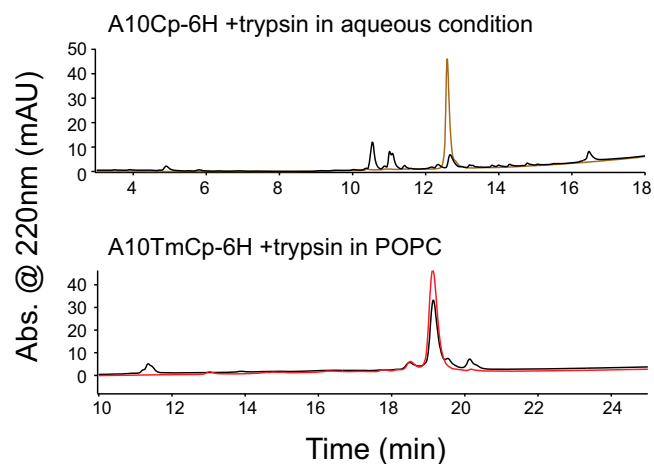


**Fig. S3.** Overlaid HPLC traces depicting the limited trypsin digestion of A10Cp-6H in aqueous solutions (*Top*) and A10TmCp-6H reconstituted in POPC liposomes (*Bottom*). A10Cp-6H stock or A10TmCp-6H in the POPC liposome was diluted into the 20 mM Tris-HCl buffer (containing 100 mM NaCl and 1 mM DTT, pH 8.0) to a final concentration of 100  $\mu$ g/mL Red trace: before trypsin was added; black: 1 h after trypsin digestion at 37  $^{\circ}$ C.

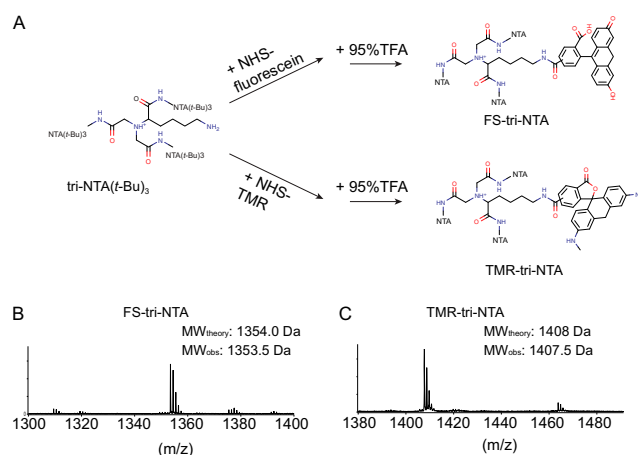


**Fig. S4.** Synthesis of FS-tri-NTA and TMR-tri-NTA. (A) Scheme of synthesis. The active primary amine group in tri-NTA(*t*-Bu)<sub>3</sub> reacts with NHS-fluorescein or NHS-TMR, followed by the removal of *t*-butyl group by 95% (vol/vol) trifluoroacetic acid (TFA). The final products were purified, lyophilized, and further analyzed by MALDI-TOF. The measured molecular masses of (B) FS-tri-NTA and (C) TMR-tri-NTA matched the predicted values.

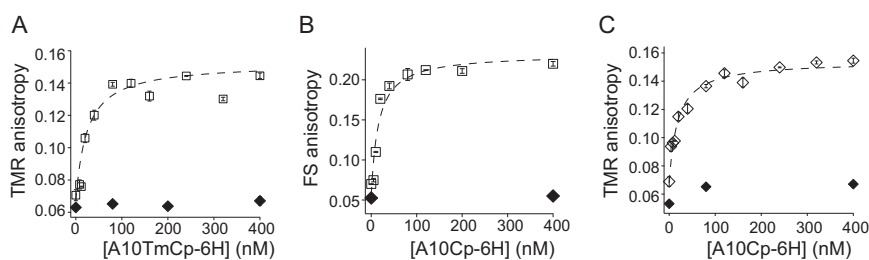


**Fig. S5.** Binding isotherms of noted fluorophore-tri-NTA with A10TmCp-6H or A10Cp-6H detected by fluorescence anisotropy. The FS-tri-NTA or TMR-tri-NTA stock solution was dissolved in the DPC micellar solution to 1 nM concentration. A10TmCp-6H or A10Cp-6H in the same solution was titrated in the presence of 1  $\mu$ M NiSO<sub>4</sub> (□) or 10 mM EDTA (♦). The change in fluorescence anisotropy of (A and C) TMR-tri-NTA and (B) FS-tri-NTA were plotted as a function of the protein concentration. The binding isotherm was fitted to the hyperbolic function (dashed lines), and the dissociation constants were summarized in Table 1.



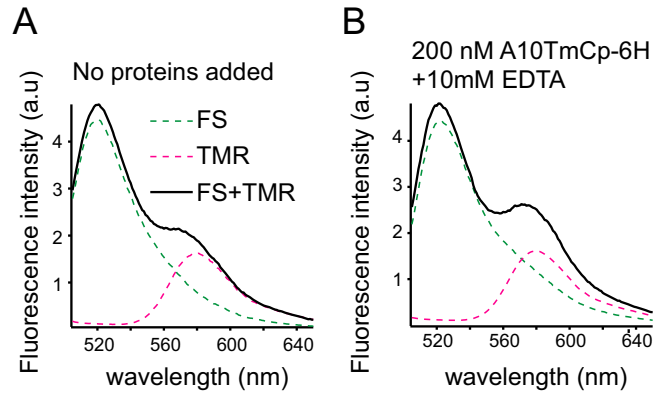


**Fig. 56.** Lack of FRET between FS-tri-NTA and TMR-tri-NTA (*A*) in the absence of any proteins or (*B*) in the presence of 200 nM A10TmCp-6H and 10 mM EDTA. The fluorescence spectra of the donor alone (green dashed line, 100 nM FS-tri-NTA), the acceptor alone (pink, 100 nM TMR-tri-NTA) and the mixture (black solid line, 100 nM FS-tri-NTA and 100 nM TMR-tri-NTA) in the DPC micellar solution were recorded with excitation at 494 nm.

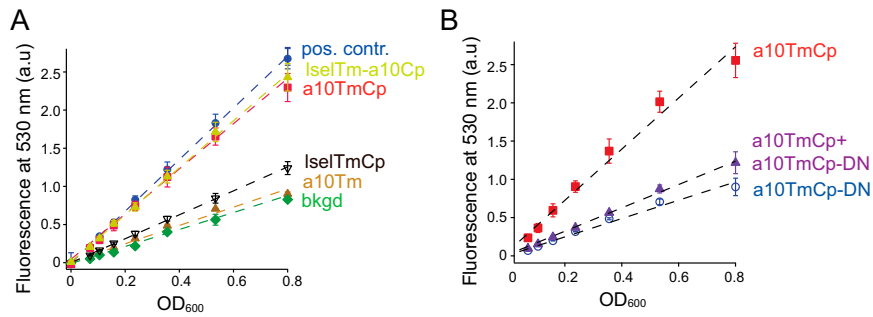


**Fig. 57.** Fluorescence intensities at 530 nm of the MBP chimeric proteins from serial dilution of bacterial cultures were plotted against the corresponding cell density ( $OD_{600}$ ). Each data point is mean  $\pm$  SD ( $n = 3$ ). Each dashed line represents the linear regression fit of the plot.

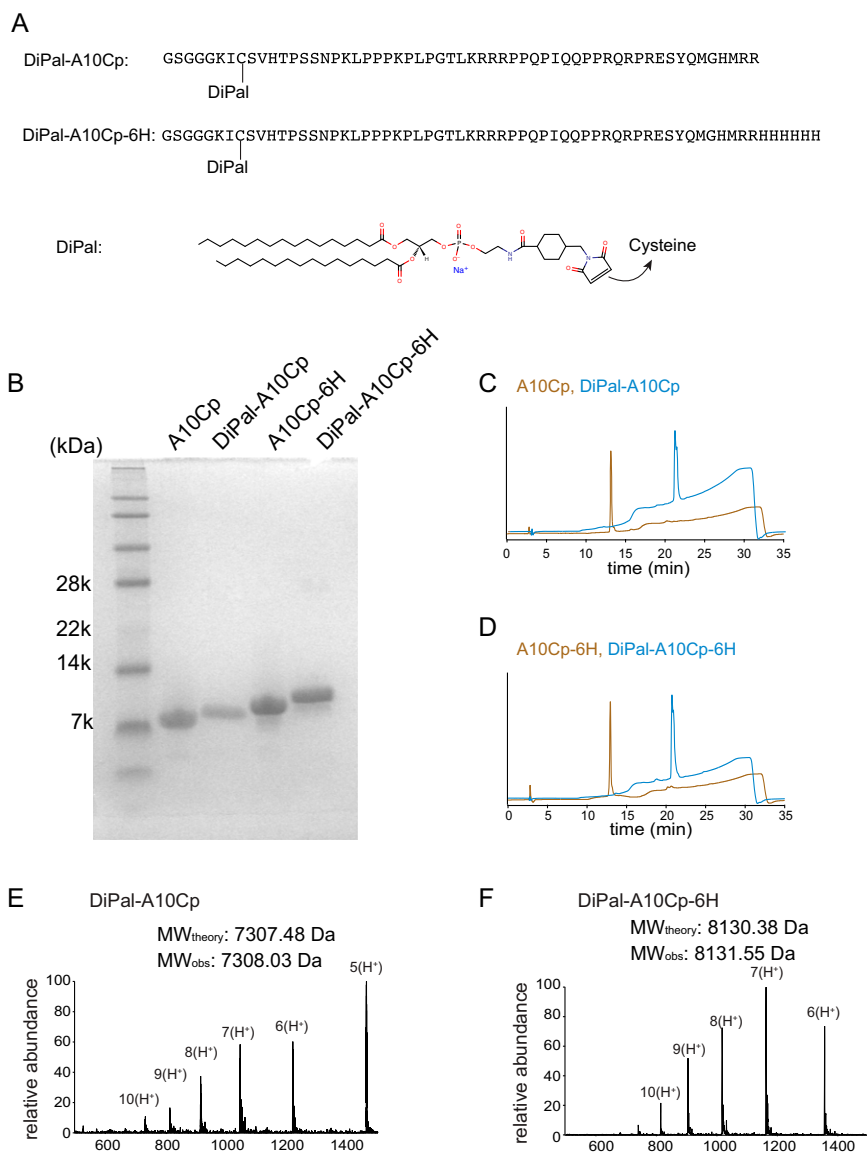


**Fig. S8.** Preparation of lipidated A10Cp. (A) Sequences of DiPal-A10Cp and DiPal-A10Cp-6H. Note the location of Cys699 to which DiPal is attached. The chemical structure of DiPal is also shown. (B) SDS gel showing the purity of DiPal-A10Cp and DiPal-A10Cp-6H. Note the slight gel shift as a result of lipidation. (C) Overlaid analytical HPLC traces of A10Cp (brown trace) and DiPal-A10Cp (blue). (D) Overlaid analytical HPLC traces of A10Cp-6H (brown trace) and DiPal-A10Cp-6H (blue). (E) Mass spectrum of DiPal-A10Cp. (F) Mass spectrum of DiPal-A10Cp-6H.

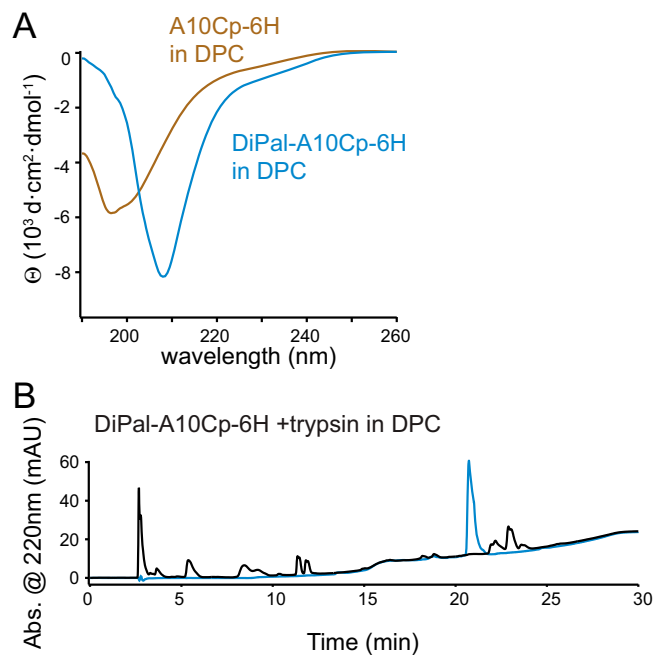


**Fig. 59.** Characterization of DiPal-A10Cp-6H in DPC micelles. (A) Overlaid CD spectra of A10Cp-6H (black trace) and DiPal-A10Cp-6H (blue) in DPC micellar solution. (B) Overlaid HPLC traces depicting the limited trypsin digestion of DiPal-A10Cp-6H in DPC micellar solution. The sample preparation was the same as Fig. S2. Blue trace, before trypsin digestion; black, 1 h after trypsin digestion at 37 °C.